STATE RESEARCH CENTER OF RUSSIA

INSTITUTE FOR HIGH ENERGY PHYSICS

IHEP 98-51

V.V.Ammosov, V.A.Gapienko, V.F.Konstantinov,
Yu.M.Sviridov, V.G.Zaets

STUDY OF AVALANCHE MODE OPERATION OF RESISTIVE PLATE CHAMBERS WITH DIFFERENT GAS GAP STRUCTURES

Submitted to *NIM*

Protvino 1998

UDK 537.613 M–24

Abstract

Ammosov V.V. et.al. Study of Avalanche Mode Operation of Resistive Plate Chambers with Different Gas Gap Structures: IHEP Preprint 98-51. – Protvino, 1998. – p. 13, figs. 8, tables 2, refs.: 9.

Operation of narrow gap, wide gap and multigap RPCs in an avalanche mode was studied. No advantage in the avalanche-streamer separation was found for the wide gap and multigap chambers operating with Ar-based mixture as compared with the narrow gap chamber. For dense tetrafluoroethane-based mixture, proportionality was observed between streamer-free plateau width and total gas thickness, in a rough agreement with the corresponding shift of the maximum of avalanche charge distributions from zero. The best result was obtained for the double-gap chamber with the read-out electrode located between two subgaps.

Аннотация

Аммосов В.В. и др. Изучение работы в лавинном режиме резистивных плоскопараллельных камер с различной структурой газового зазора: Препринт ИФВЭ 98-51. – Протвино, 1998. – 13 с., 8 рис., 2 табл., библиогр.: 9.

Изучена работа узкозазорных, широкозазорных и многозазорных РПК в лавинном режиме. Не обнаружено преимуществ широкозазорных и многозазорных камер, работающих с газовой смесью на основе аргона, перед узкозазорными в отношении разделения областей лавинного и стримерного режимов. Для плотной смеси на основе тетрафторэтана наблюдалась пропорциональность между шириной бесстримерной области плато эффективности и полной толщиной газа, в качественном согласии с соответствующим сдвигом от нулевого значения наиболее вероятной величины заряда лавины. Наилучший результат получен для двухзазорной камеры с сигнальным электродом, расположенным между двумя зазорами.

INTRODUCTION

In the both general-purpose LHC detectors the Resistive Plate Chambers are proposed as one of the base detectors for the muon trigger system [1,2]. Because of a large expected background these RPCs should operate in the so called avalanche mode, which provides higher rate capability and stable timing properties independent of counting rate. To compensate for low gas gain (as compared with streamer mode) the RPC should be equipped with high gain amplifiers and low threshold discriminators. In these conditions the appearence of streamers with even low probability is utterly undesirable. Streamer signals are about 100 times higher than avalanche ones, and they can cause the firing of several read-out strips per single throughgoing particle and a considerable increase in the detector dead time. Thus one of the problems connected with the use of RPC in the avalanche mode is the existence of a wide enough region in the applied HV, in which one can achieve the full efficiency of an RPC while keeping the streamer fraction negligible.

Two ways to solve this problem are currently under study. One way is the search for more suitable (in particular more dense and quenching) gas mixture for traditional narrow (about 2 mm) gas gaps [3]. The other one is oriented to developing alternative RPC geometrical designs — double-gap [2], wide gap [4] and multigap [5] chambers. In all these approaches the general idea consists in improving the avalanche charge distribution, that is in obtaining the distributions with non-zero maximum and reduced tailes. The second goal is to reduce the number of electrons needed to produce a given fast signal in the external read-out circuit, in other words, to reduce gas gain coefficient G.

In this paper we present the results of the study of avalanche-streamer separation for different RPC structures and two gas mixtures.

Let us recall briefly the general principles of RPC operation and the motivations for the above-mentioned approaches. RPC is a gaseous detector with electron multiplication in gas gap of width d enclosed by two parallel HV electrodes made of dielectric (bakelite) with bulk resistivity of about 10^{10}-10^{12} Ohm·cm. HV is spread over outer surfaces of bakelite with the use of conductive paint. An avalanche produced in gas gap induces signal on read-out electrodes placed on both sides of the detector. In multigap chambers,

gas gap is additionally divided by bakelite sheets to form several subgaps; in proposed scheme [5], these additional HV electrodes are floating. In the double-gap chamber, read-out electrode is placed between two subgaps.

A total charge of electrons contained in an avalanche (avalanche size) produced by a charged particle traversing gas gap d can be expressed as

$$Q = q_e \sum n_i \times exp[\beta(d - x_i)]. \tag{1}$$

Here x_i is the distance from the cathode of the production point of i-th cluster of multiplicity n_i and β is the effective first Townsend coefficient equal to the difference between multiplication α and attachment η coefficients; q_e-electron charge. Summation is carried out on all clusters in the gap. The average avalanche size Q_g can be obtained from (1) as

$$Q_g \simeq q_e(\nu n d)e^{\beta d}/\beta d, \tag{2}$$

where n is average cluster multiplicity, ν — primary cluster density.

A fast signal, induced in read-out circuit, is related to the avalanche size, according to the Ramo-Shockley theorem, as

$$q \simeq QE^*/\beta \equiv Q/\beta D. \tag{3}$$

Here E^* is the conditional field strength in gas gap for the case when pick-up electrode of interest has unit potential and all other conductive electrodes are grounded. For the parallel plate geometry, E^* is constant and one can write in this case $E^* = 1/D$, where D can be called "effective total gap width".

Using the continuity condition for electric displacement, one can obtain for the real RPC structure

$$D = kd + (\frac{t_b}{\varepsilon_b} + \frac{t_m}{\varepsilon_m}) \tag{4}$$

for the chamber of k subgaps of the width d. Here t_b, t_m are the total bakelite and mylar thickness between two opposite read-out electrodes and ε_b, ε_m — their relative permittivities.

If one can consider each subgap of a k-gaps chamber as independent and keeping exactly 1/k-th of applied voltage, then it is natural to write down

$$q \simeq kQ_g/\beta D, \tag{5}$$

where Q_g is, in this case, the average avalanche size in a subgap.

From (1) it follows, that for low primary cluster density, only few clusters contribute to the sum, because of the very sharp dependence of Q on $(d\text{-}x_i)$. For 2 mm gap chamber working with Ar-based mixture, first two clusters account, in average, for 90% of the resulting signal [6]. Therefore, the size of particular avalanche is very sensitive to the coordinate of the first cluster formation, especially for narrow gaps. For gases with higher primary cluster density more clusters can contribute to the sum, reducing fluctuations in the resulting avalanche size and shifting mean avalanche charge to higher values, for the given gas gain (see also [7]).

For wide gap chambers the same effect of increasing "useful" number of clusters is achieved by increasing gap width. Further, because a mean avalanche size is goverened primarily by $\exp(\beta d)$, the (βd)-values should be approximately equal for all kinds of

chambers, and in the case of wide gaps, one could hope to operate at lower values of β approximately in the ratio

$$\beta_2 \simeq \beta_1 d_1/d_2, \tag{6}$$

where β_1,β_2 refer to gap widths d_1, d_2, respectively. Thus, one can hope to reduce further one of the sources of avalanche size fluctuations.

For the multigap chambers the measured signal is determined by the sum of avalanches produced in all subgaps. Accordingly, the fluctuations of the resulting signal are expected to be lower.

From relations (4) and (5) one can see, that neither wide gap nor multigap chambers are capable to provide a lower avalanche size in gap/subgap for the given measured signal q. We can rewrite expression (5) in the form

$$q \simeq (k/r)Q_g/\beta d, \tag{7}$$

where r = D/d. Coefficients (k/r) are contained for our monogap and multigap chambers in the range from 0.83 for 6.3 mm monogap chamber to 0.56 for 3×0.7 mm RPC, compared with (k/r) = 0.71 for 2.1 mm narrow gap chamber, so the ratios q/Q_g differ only slightly for these chambers. For double-gap chamber, k = 1 in (4), due to electrode location between subgaps, but k = 2 in (5), and thanks to this feature (k/r) = 1.43 in (7). Thus only double-gap chamber can, in principle, realize both advantages: about two times lower avalanche size in each subgap and reduction of avalanche fluctuations due to summing signals from both subgaps.

Of course, this picture of RPC operation is simplified because in the region of high gas amplification space charge effects should be taken into account. The role of the electronegativity of the gases used is also not understood in details yet [8].

1. EXPERIMENTAL SET-UP

Measurments were made at the test facility of the IHEP U-70 accelerator in the beam of low momentum (a few GeV) positive particles, mostly hadrons. A full width of the beam at half maximum at detectors position was about 20 cm. The experimental set-up is shown on Fig.1-a. Trigger was worked out by five-fold coincidence of scintillation counters S1–S5 and picked out 1.5×4 cm^2 area of detectors. The trigger rate varied from 15–20 up to 300 triggers per spill (spill length 0.5–0.8 s). The test area had high background irradiation from the main ring and nearby placed targets of other channels. This background rate was determined with the use of scintillation counter to be about 100 Hz/cm^2 throughout the run.

The following set of detectors was installed in the beam:

1) 0.5 × 2 m^2 large RPC module, containing two independent chambers, one having 2.1 mm wide gap and the other – 4.1 mm. Each chamber had X and Y read-out strip panels, strip width being 28 mm with 30 mm pitch.

2) 30 × 30 cm^2 test module (TM), containing three chambers: 2.3 mm and 6.3 mm monogap RPCs and 3 × 2.3 mm multigap chamber. Each chamber had X and Y read-out strips similar to the large RPC module. This module was specially made for the comparative study of the narrow and wide monogaps and multigap RPCs.
3) Several small (80 cm^2 sensitive area) test RPCs were studied in the gas tight box (GB):

   1.7 mm, 3.0 mm and 3.8 mm monogap chambers;
   3 × 1.5 mm, 3 × 1.0 mm and 3 × 0.7 mm multigap ones and
   2 × 2.3 mm double-gap chamber with read-out pad located between two sub-gaps.

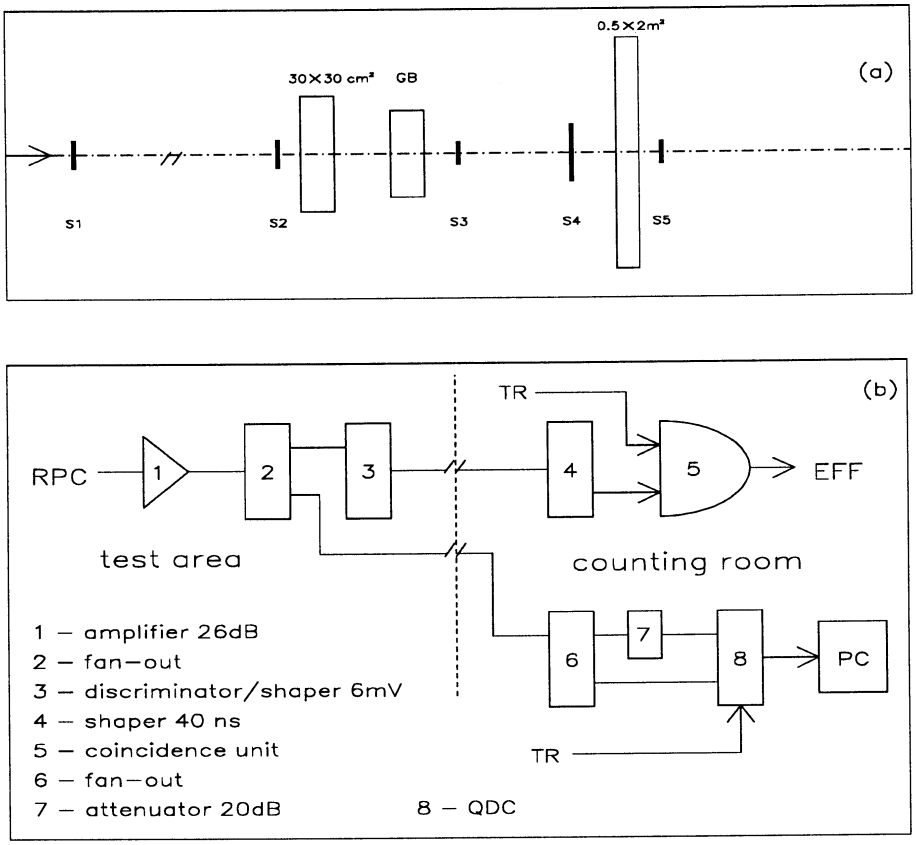

Fig. 1. Experimental set-up: a — detectors lay-out , b — baseline circuit for charge measurements.

Inner electrodes for multigap chambers were made of 0.8 mm thick melamine-phenol-melamine sheets with volume resistivity of about 10^{13} Ohm cm; for all other electrodes 1.6 mm thick phenol-melamine plates were used having (1-3)×10^{12} Ohm·cm volume resistivity. No additional treatment was applied to the inner surfaces of gas gaps. In the multigap chambers, HV was applied only to outer electrodes, thus inner electrodes were floating.

Gas flowed in succession through two gaps of the large RPC, three chambers of the TM and then through the GB with flow rate 75 cm^3/min. We used two gas mixtures. Most of the data were obtained with two-component mixture based on tetrafluoroethane (TFE) with admixture of 6% of isobutane [9] (heavy mixture, estimated cluster density about 7 mm^{-1}). A direct comparision of the three chambers of the TM turned out to be possible, however, only for Ar-enriched mixture Ar/TFE/isobutane = 74/20/6 (light mixture, ν =3.5 mm^{-1}) due to HV source limitation.

We used as a base a commercial amplifier U3-33 with 26 dB amplification and 400 MHz band width. The amplified signal was sent to fan-out (Fig. 1-b). One output of fan-out through 6 mV home-made discriminator/shaper was used for efficiency and singles counting rate measurements, the other — for charge measurements with the use of QDC with 0.25 pC/count. Most of the charge data were obtained for 100 ns QDC gate.

For the large RPC strip-line impedance was measured to be 12 Ohm. Far ends of all strips were terminated with 12 Ohm resistors, therefore, only 20% of fast charge was measured with 50 Ohm input impedance amplifier. On the other hand, the read-out pads in the GB were loaded by 1 kOhm resistors, as well as the strips of the TM chambers. Hence, all fast induced charge was measured in these cases.

The circuit sensitivity with respect to the amplifier input was measured to be 25 fC/count for unattenuated signals. With 20 times amplification and 6 mV discrimination threshold, we had the threshold reduced to RPC output of about 0.3 mV. We estimated our threshold charge to be about 50 fC.

Streamer probability was determined from the measured charge spectra as a fraction of events contained in a peak or cluster which was visibly separated from the avalanche tail.

2. RESULTS AND DISCUSSION

Efficiency and streamer fraction. Summary of experimental results for both gas mixtures is presented in Table 1. In this Table the plateau knee voltage V_0 is defined as the voltage above which the efficiency does not rise further.

A direct comparision of different RPC structures was made for the Test Module chambers for the light gas mixture Ar/TFE/isobutane = 74/20/6. The results on efficiency and streamer fraction are shown on Fig. 2 as a function of field strength E=V/d_{tot}, where d_{tot} = kd. As it is seen from the data, the efficiency for the narrow gap chamber does not exceed 90%. Streamers are observed already at the plateau knee at the level of 1%, and their probability increases rapidly. For the wide gap and multigap chambers the efficiency is higher, but not sufficiently. The wide gap chamber shows some streamer-free region, about 100 V on the plateau, with the streamer fraction f_s less than 1%. But for this chamber the efficiency curve has an observable inverse slope. This effect is known and usually referred to high resistivity of bakelite. It is seen from the data that the wide gap RPC turned out to be most sensitive to these effects. Processes that cause efficiency decrease with HV increasing can hinder, at the same time, the streamer formation. Thus, the result on the streamer suppression for the wide gap chamber should be taken with care.

Table 1. General characteristics of studied RPCs

RPC type	V_0,kV	ε,%	f_{knee},%	q_{knee},pC	ΔV,V
light mixture					
2.3 mm	6.0	89.3±0.5	0.5	0.5	<100
6.3 mm	13.4	94.4±1.0	0.0	1.2	100
3 × 2.3 mm	17.5	96.8±0.5	1.2	0.5	–
heavy mixture					
1.7 mm	8.1	96.2±0.6	6.6	1.6	–
2.1 mm	9.5	97.6±0.1	0.7	1.8	<100
2.3 mm	10.1	98.7±0.1	0.05	0.9	200
3.8 mm	14.2	97.4±0.4	0.0	1.3	400
3 × 1.0 mm	14.0	99.5±0.3	0.24	0.9	200
3 × 1.5 mm	16.8	99.8±0.2	0.13	0.9	400
2 × 2.3 mm	9.9	99.8±0.1	0.0	1.1	350

V_0 – plateau knee voltage, ε – average efficiency on the plateau, f_{knee} – streamer fraction at plateau knee, q_{knee} – measured avalanche charge at the knee, ΔV – plateau width with streamer fraction less than 1%.

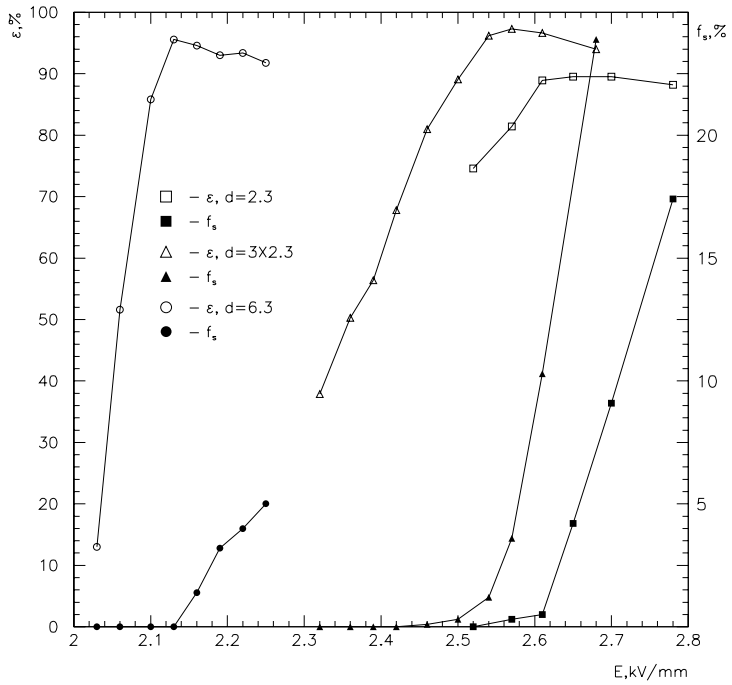

Fig. 2. 30 × 30 cm^2 module, light gas mixture Ar/TFE/isobutane = 74/20/6. Efficiency ε and streamer fraction f_s vs field strength.

For the multigap chamber no streamer-free plateau region was observed at all.

All other results presented were obtained for heavy gas mixture. The effect of this mixture is clearly seen from Fig.3, where efficiencies and streamer fractions for the 2.3 mm

monogap chamber are compared for both gases. For the heavy mixture the efficiency is higher than 98% for at least 400 V plateau, and, most important for our study, about 200 V wide region of the plateau with f_s<1% is seen.

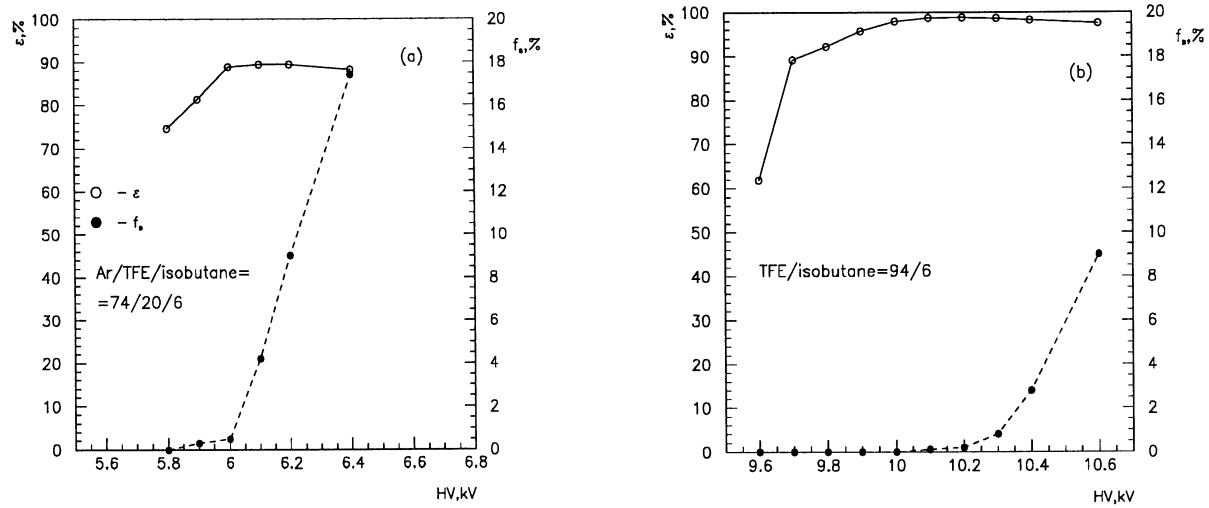

Fig. 3. 30 × 30 cm^2 module, 2.3 mm gap. Efficiency and streamer fraction vs HV for (a) light Ar/TFE/isobutane = 74/20/6 and (b) heavy TFE/isobutane = 94/6 gas mixtures.

Efficiencies and streamer probabilities for some RPC studied with heavy mixture are presented on Fig. 4 as a function of E.

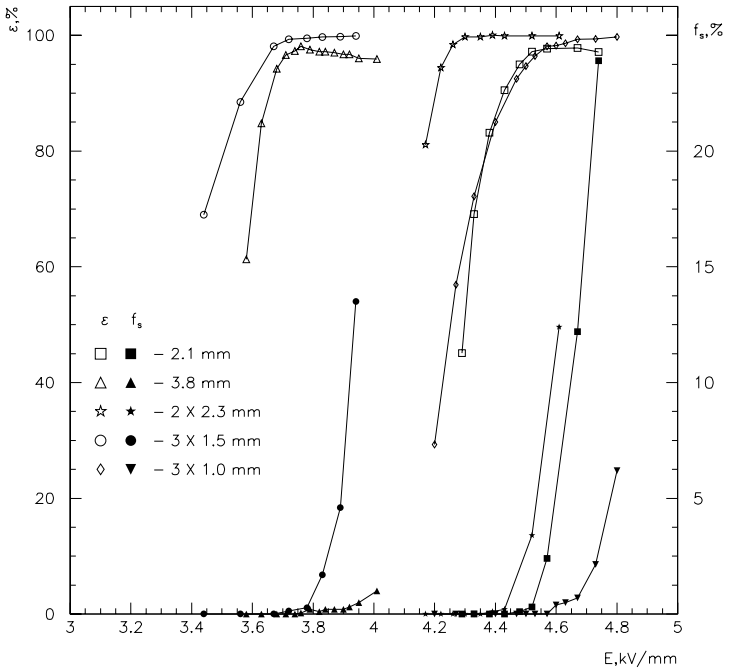

Fig. 4. Efficiency and streamer fraction as a function of field strength E for narrow gap, wide gap, multigap and double-gap chambers for heavy mixture.

For 2.1 mm gap of large chamber efficiency reaches about 98%, but the plateau region with streamer fraction less than 1% is too narrow, less than 100 V.

We studied two "wide" gap, 3.0 and 3.8 mm RPCs with heavy mixture. Main characteristics — efficiency and streamer probability for the 3.8 mm wide gap chamber are shown in Fig.4 and Table 1. A visible streamer-free region of about 400 V is seen. But we observed relatively low peak value of efficiency comparable with the efficiency of narrow gap RPCs. Moreover, a visible inverse slope of the efficiency curve with HV increasing is clearly seen. Such effect has already been mentioned in the discussion of the wide gap (6.3 mm) chamber with light mixture. Our conclusion in the case of 3.8 mm gap RPC is the same: streamers suppression is the consequence of high sensitivity of wide gap RPCs to the details of chamber constraction and operating conditions, in particular, to bakelite resistivity and counting rate.

Another effect was also observed for this chamber: streamer fraction is about three times higher when using 250 ns QDC gate. For 500 ns gate width, streamer probability does not rise further. But an average streamer charge increases approximately linearly with the gate width up to 500 ns.

To study multigap RPC performance with heavy mixture we have made three small set-ups for GB: 3 × 1.5 mm, 3 × 1.0 mm and 3 × 0.7 mm.

Efficiency and streamer probability as a function of field strength for 3 × 1.5 mm and 3 × 1.0 mm chambers are shown on Fig.4; relevant data for these chambers are also listed in Table 1. First of all the plateau efficiency is > 99% for both chambers. The 3 × 1.0 mm and 3 × 1.5 mm chambers show 200 V and 400 V wide gaps between plateau knee and 1% streamer onset, respectively. But in this case too streamers at $\simeq 0.1\%$ probability level occur already at the plateau knee.

Best result was obtained for another type of multigap RPC — double-gap 2 × 2.3 mm chamber with read-out electrode located between two subgaps (see Fig. 4). There is seen 350 V wide region on the plateau with f_s<1% for both 100 and 250 ns QDC strobes and about 200 V — with streamer fraction less than 0.1 %. A total plateau width with efficiency greater than 99% is more than 1 kV. Such result is, to our mind, the consequence of the features of this type of RPC mentioned in the Introduction.

Some relevant quantities, that characterize operation mode of RPCs of different designs, are presented in Table 2. These quantities refer to equal measured charges q = 1.1 pC (average for these chambers at plateau knee, q_{knee} = 1.1±0.2 pC, see Table 1). This Table confirmes some statements made above:

1. For all chambers, βd-values are approximately the same.

2. For wide (3.8 mm) gap RPC the value of β is lower than for narrow 2.3 mm gap (see (6)).

3. Average avalanche size in each subgap of multigap chamber is the same as for narrow and wide monogaps.

4. Only double-gap chamber realizes completely the advantages of two subgaps: avalanche size in each subgap is more than two times lower than for all other chambers.

Table 2. Gas multiplication parameters for different kinds of RPCs

RPC type	βd	β,mm^{-1}	βD	Q_g,pC	G
2.3 mm	18.3	7.9	25.6	30.7	8.9×10^7
3.8 mm	17.6	4.7	22.8	27.4	4.4×10^7
3×1.5 mm	18.7	12.5	74.8	29.9	1.3×10^8
2×2.3 mm	16.7	7.3	23.5	11.7	1.8×10^7

d – gap or subgap width for monogap and multigap chambers, respectively, β – effective first Townsend coefficient, D – effective total gap width, Q_g – avalanche charge in gas gap/subgap, G – gas gain coefficient.

Charge distributions. Charge spectra were measured for all the chambers. Two representative distributions are shown on Fig. 5 for 1.7 mm monogap chamber and for double-gap RPC, at mean charge values of around 1 pC. Different behaviour of charge distributions is clearly seen. While for the 1.7 mm chamber we have an exponential distribution, the double-gap chamber shows a "Landau-like" shape of charge spectrum with maximum well separated from zero.

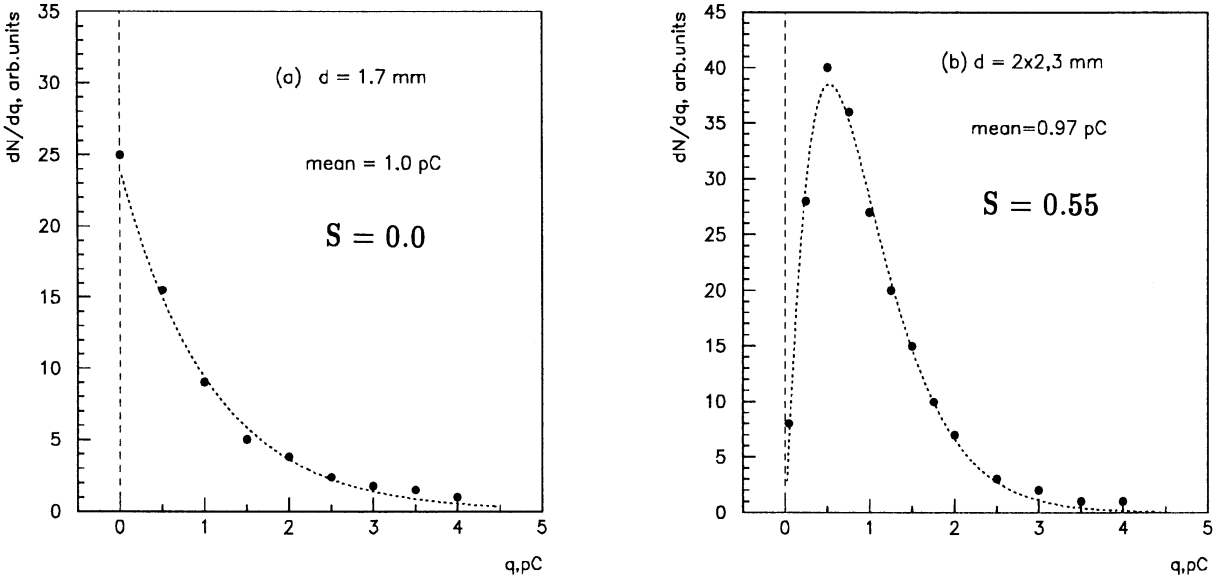

Fig. 5. Measured charge spectra in avalanche region for (a) 1.7 mm monogap chamber and (b) for CMS-type double-gap RPC, for heavy gas mixture.

To study more quantitatively measured charge distributions, these spectra were fitted for all the chambers with the Polya-like relation

$$dN/dq \sim q^{(b-1)} exp(-bq/q_0) \tag{8}$$

Here q_0 is a mean charge and b is a parameter. Resulting approximations for two chambers are shown by dotted curves on Fig. 5.

We defined a "symmetry parameter"

$$S = q_{mp}/q_0, \tag{9}$$

where q_{mp} is the most probable charge values. Obviously, the limiting values for S are 0 for the exponential shape of charge spectrum and 1 for the symmetrical "Gaussian-like" one. On Fig.6, the obtained values of S for all chambers are shown as a function of total gas gap thickness d_{tot} = kd. For both gas mixtures, S increases with the total gas thickness. The slope of this rise is higher for heavy gas. This observation can be interpreted as an indication that the total primary ionization and its density exerts a main influence on the shape of an avalanche distribution in our conditions. Curves on this figure are the results of the fit to experimental points of the function

$$S = 1 - exp(-a(d_{tot} - d_{tot0})), \tag{10}$$

which satisfies qualitatively limiting conditions expected for S.

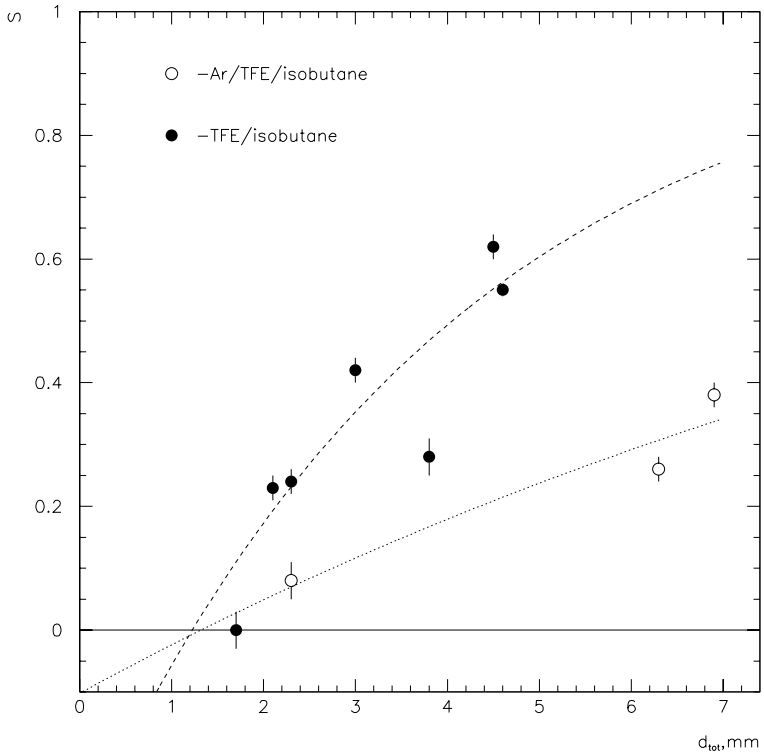

Fig. 6. Symmetry parameter S as a function of gas thickness d_{tot}.

On Fig.7 the pure avalanche plateau width ΔV is plotted vs d_{tot} for both mixtures. Comparision of this figure with Fig.6 shows that for the TFE-based mixture both ΔV and S increase with the total gas thickness in a similar way. Thus, for this mixture the width of streamer-free region corresponds, at least qualitatively, to the improvement in avalanche charge distribution shape.

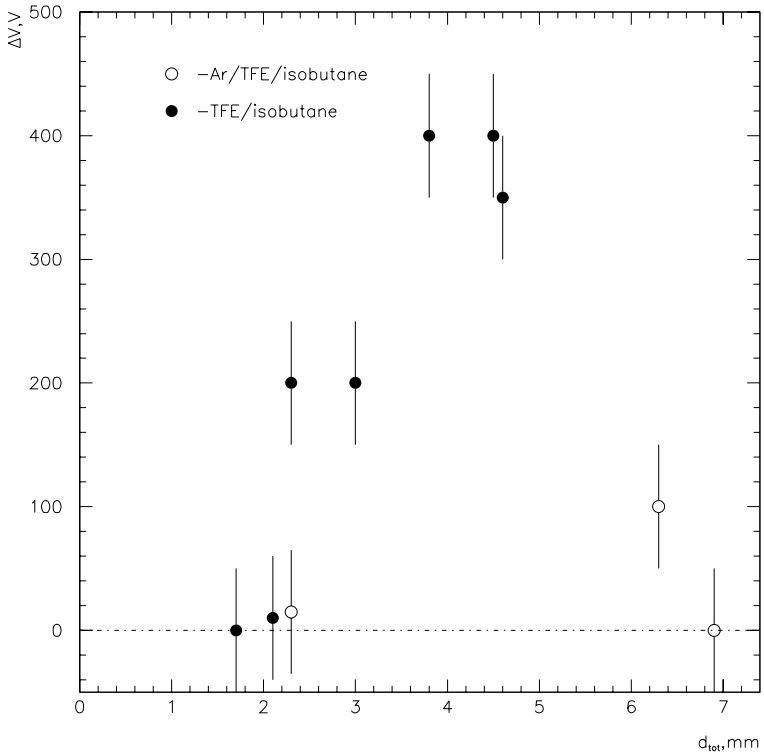

Fig. 7. Pure avalanche plateau width ΔV as a function d_{tot}.

This is not the case for Ar-based mixture: a visible increase of symmetry parameter for wide gap and multigap chambers renders no influence on the avalanche-streamer separation. Evidently, the quenching ability of this mixture is too weak.

Using relations (2), (3) and (4) and experimental data for monogaps, we estimated β values for a relatively wide range of field strength E (Fig.8). We used here $\nu = 7$ mm^{-1} for the heavy mixture and $\nu = 3.5$ mm^{-1} for the light one, and n = 3. These dependences can be satisfactorily fitted with the form

$$\beta(cm^{-1}) \simeq 1450 exp(-12.6/E(kV/mm)) \tag{11}$$

for the heavy mixture and

$$\beta(cm^{-1}) \simeq 5320 exp(-11.1/E(kV/mm)) \tag{12}$$

for the light one.

We should make some remarks concerning the multigap chambers. Defining field strength in each subgap as E = V/kd and using the corresponding values of β, we cannot reproduce the measured charges, for the TFE-based mixture. In fact, for the 3×1.5 mm chamber the plateau knee field strength E_0 is 3.73 kV/mm, and $\beta(E_0) \simeq 4.95$ mm^{-1}. Accordingly, q_{knee} can be estimated as 0.1 fC, four orders of magnitude lower than the measured value. For Ar-based mixture, $E_0 = 2.54$ kV/mm, $\beta \simeq 6.73$ mm^{-1} and $q_{knee} \simeq$ 0.7 pC, in agreement with the observed value. We cannot explain this contradiction.

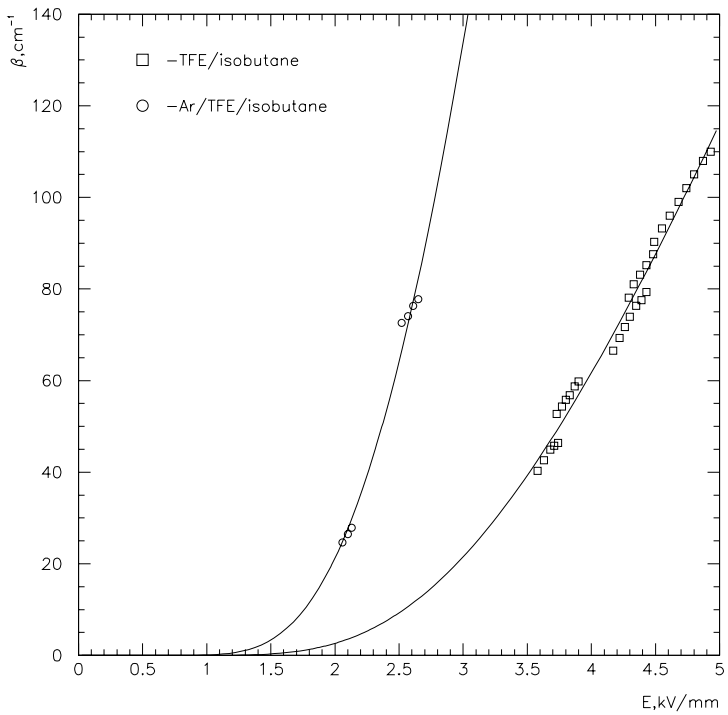

Fig. 8. An estimate of the effective first Townsend coefficient.

CONCLUSION

We studied the avalanche-to-streamer transition for different RPC geometrical schemes in order to find the best one with respect to a high efficiency in the avalanche mode and at the same time a low streamer probability for the wide enough efficiency plateau region. Our conclusions are summarized below:

1. For the light Ar-enriched mixture all the RPC structures studied (narrow gap, wide gap and multigap) do not show any practical streamer-free region.

2. For tetrafluoroethane-based mixture, the pure avalanche plateau width seems to grow with the total gas thickness.

3. The increase of the avalanche plateau width with total gas thickness for TFE-based mixture is in agreement with the corresponding shifting from zero of the most probable values of avalanche charges. No relationship was observed between the avalanche charge distribution shape and avalanche-streamer separation for Ar-based mixture.

4. The best result was obtained for the double-gap chamber with read-out electrode located between two subgaps, for TFE-based mixture: about 200 V wide pure avalanche plateau with the streamer fraction less than 0.1% and $> 99\%$ efficiency.

5. Some characteristics of the RPC operation mode and gas mixtures properties were also estimated: the avalanche size in gas gap or subgap, gas gain coefficients at the plateau knee and the dependence of the effective first Townsend coefficient on the applied electric field for two gas mixtures.

Our results for two gas mixtures and different gas gap structures indicate that the search for a new more suitable gas mixture is the most promising way to solve the problem of stable RPC operation in a pure avalanche mode.

ACKNOWLEDGEMENTS

The authors would like to thank C.Fabjan, R.Santonico and R.Cardarelli for their interest to our work. We are especially grateful to M.C.S.Williams for fruitful discussions and continuous support. We also wish to thank A.Golovin and N.Mishina for hard work on RPCs manufacturing.

References

[1] ATLAS Technical Design Report.Muon Spectrometer. – CERN/LHCC 97 – 22,Geneva,1997.

[2] The CMS Technical Proposal. CERN/LHCC/94 – 38, LHCC/P1 (1994).

[3] A.Di Ciaccio.Nucl. Instr. Meth. A384 (1996),22.

[4] I.Crotty et al. Nucl. Instr. Meth. A360 (1995),512; E.Cerron Zeballos et al. Nucl. Instr. Meth. A367 (1995),388.

[5] E.Cerron Zeballos et al. "New Type of Resistive Plate Chamber: The Multigap Chamber." CERN PPE/95 – 166, CERN/LAA – MC95 – 23, Geneva, 1995; E.Cerron Zeballos et al., Nucl. Instr. Meth. A392 (1997), 145; M.C.S. Williams. Nucl. Phys. B (Proc. Suppl.) 61B (1998), 250.

[6] M.Abbrescia et al., Nucl. Instr. Meth. A398 (1997), 173.

[7] M.Abbrescia et al., Nucl. Instr. Meth. A392 (1997), 155.

[8] P.Camarri et al.,"Streamer suppression with SF_6 in RPCs operated in avalanche mode", ATLAS Internal Note MUON-NO-226, 1998.

[9] R.Cardarelli, V.Makeev, R.Santonico. Nucl.Instr.Meth A382 (1996), 470.

Received July 29, 1998

В.В.Аммосов и др.
Изучение работы в лавинном режиме резистивных плоскопараллельных камер.

Оригинал-макет подготовлен с помощью системы LaTeX.
Редактор Е.Н.Горина. Технический редактор Н.В.Орлова.

Подписано к печати 3.08.98. Формат 60 × 84/8. Офсетная печать.
Печ.л. 1.62. Уч.-изд.л. 1.24. Тираж 180. Заказ 253. Индекс 3649.
ЛР №020498 17.04.97.

ГНЦ РФ Институт физики высоких энергий
142284, Протвино Московской обл.

Индекс 3649

П Р Е П Р И Н Т 98-51, И Ф В Э, 1998